Perpendicular standing spin waves in films with interfacial Dzyaloshinskii-Moriya interaction

Ellen Lu
School of Information and Physical Sciences, The University of Newcastle, Callaghan, NSW, 2308 Australia

Kristen S. Buchanan
Department of Physics, Colorado State University, Fort Collins, Colorado, USA.

Karen L. Livesey
School of Information and Physical Sciences, The University of Newcastle, Callaghan, NSW, 2308 Australia and Biofrontiers Center, University of Colorado Colorado Springs, Colorado Springs, Colorado, 80918 USA.

(Dated: December 12, 2024)

The interfacial Dzyaloshinskii-Moriya interaction (DMI) is known to induce non-reciprocity in spin wave propagation within the plane of magnetic thin films. This non-reciprocity can be utilised to design spin wave devices such as signal isolators, and also provides an important means to quantitatively measure the magnitude of the DMI. Analytical expressions have been developed to estimate the effects of DMI on spin waves by assuming the magnetization dynamics are uniform throughout a film thickness. Here, we relax this assumption and use a so-called 'atomic layer method' to calculate spin wave dispersion relations for not just the uniform thickness mode, but also for the perpendicular standing spin waves (PSSWs). Coupled magnetic equations of motion are written for each atomic plane within a thin film made of one or more materials. The method is tested against known analytic and numerical theories, and is then used to calculate the PSSW frequencies and mode profiles for single and bilayer magnetic films with interfacial DMI applied to the outer interfaces. These calculations show that the PSSW mode frequencies depend nonlinearly on the interfacial DMI strength and on the inverse thicknesses of the magnetic films. We develop an analytic estimate for the lowest two PSSW frequencies to explain this nonlinear dependence. Our method has the advantage that it can be used to calculate spin waves frequencies and depth profiles in any thin film magnetic stack with atomic-scale variations in magnetic parameters, such as multiple DMI interfaces, or gradient properties.

I. INTRODUCTION

The Dzyaloshinskii-Moriya interaction (DMI) is a higher-order, antisymmetric exchange interaction which leads to interesting behavior in magnetic materials including the stabilization of chiral spin textures and nonreciprocal spin wave propagation. [1] Although discovered originally in bulk systems, [2, 3] this century the DMI was found to be stronger at particular magnetic interfaces. [4–7] The so-called interfacial DMI (iDMI) is particularly large at the interface between a heavy metal with strong spin-orbit coupling and a transition metal ferromagnet. [1, 8]

Spin waves are the fundamental excitations of magnetic materials. They are important for probing materials and determining the properties of hidden interfaces, [9] including those with DMI. [10, 11] They also have many applications such as spin wave logic, [12, 13] computing architectures, [14] and high-frequency signal processing. [15, 16]

Spin waves in thin films are affected by interfacial DMI, leading to exciting phenomena such as nonreciprocal propagation, [7] spin wave focusing, [17] and even the loss of standing wave modes. [18, 19] Spin waves also provide an important tool to measure the DMI experimentally. [20, 21] In most cases, theoretical studies of spin waves affected by DMI have assumed that the magnetization is uniform through the magnetic film's thickness. [22, 23] In this article, we investigate how higher-order perpendicular standing spin waves (PSSWs) are affected by interfacial DMI. In other words, we move beyond the approximation that magnetization in a thin film must be uniform with depth. This is especially important to consider in thicker films with DMI and those with multiple DMI interfaces, with multiple ferromagnetic layers, [24] or gradients in magnetic properties, [25] all of which are of increasing research interest.

One article that considered how interfacial DMI affects dynamic magnetization through a film's thickness is by Kostylev. [26] There, the interface DMI boundary condition for dynamic magnetization was derived, in analogy to the Rado-Weertman exchange boundary condition. [27] This model treats the magnetization as a continuous field, defined at all positions in space. We therefore refer to this method as the "continuum model" throughout the rest of the text. It is possible to incorporate the non-uniform thickness response of PSSWs using the continuum model, although Ref. [26] focused on the uniform mode in the Damon-Eshbach geometry (in-plane wavevector perpendicular to the in-plane equilibrium magnetization).

It is, however, difficult to extend the continuum model with DMI boundary condition to magnetic films containing multiple materials or gradients of magnetic prop-

erties. Here we instead use an "atomic layer model" whereby all magnetic properties are defined at discrete atomic layers, allowing any thin film stack to be examined. This method also allows the DMI energy to be defined only at specific interfacial atomic layers, removing the need for an effective DMI boundary condition for a continuous magnetization field.

What we are calling the "atomic layer model" is well developed for calculating PSSWs. [28, 29] It involves writing magnetization equations of motion for each atomic layer within a thin film stack, linearizing those equations, and then solving the linear system of equations to find resonant frequencies and corresponding PSSW mode profiles. The atomic layer method has been used to treat antiferromagnetically coupled stacks of thin films, [30] exchange spring bilayers, [31] and thin films with magnetoelectric coupling at interfaces. [32] Here, this method is applied to systems with iDMI. In this article, we will compare the results of using atomic layers to those of the continuum model, noting the main differences. We use the atomic layer method to show that the iDMI has substantial effects on the uniform modes in multilayers with two magnetic materials, and on PSSW modes.

We also present in the Appendix an analytic expression for frequencies of the uniform mode and first-exchange PSSW, found by treating a magnetic stack as made up of just two effective slabs. A similar approach was used recently by Yang *et al.* [33] to demonstrate that equal but opposite DMI at the top and bottom interfaces can lead to a frequency shift that is symmetric in k but in the forward volume geometry where the film is saturated out-of-plane. Our calculations show that the response is richer for the in-plane magnetization geometry, and the analytic expression supports the results of the atomic layer method calculations while providing additional insight.

Fig. 1 shows an example multilayer structure that consists of two ferromagnetic (FM) material layers in the middle of a thin film. A layer of heavy metal (HM, high spin-orbit material) is on both the top and bottom of the ferromagnetic layers in this example. Although two FM materials and two DMI interfaces are shown in this example, we also consider other material combinations in this article, including a single FM material to compare to existing theoretical works. However, the overall geometry is the same. The y direction points out-of-plane. PSSWs will therefore have amplitude variation in the y direction. We consider that the magnetic material comprises N atomic layers with $i = 1$ denoting the top atomic layer (a DMI interface as shown) and $i = N$ denoting the bottom layer. The layers labeled "DMI interface" are magnetic layers that include the interfacial DMI effects due to the adjacent heavy metal layer.

An applied magnetic field $\vec{H}$ is applied in the in-plane z direction, keeping the equilibrium magnetization in that direction. As well as magnetization variation in the thickness y direction, we also consider in-plane spin wave propagation along x, since in this direction the DMI

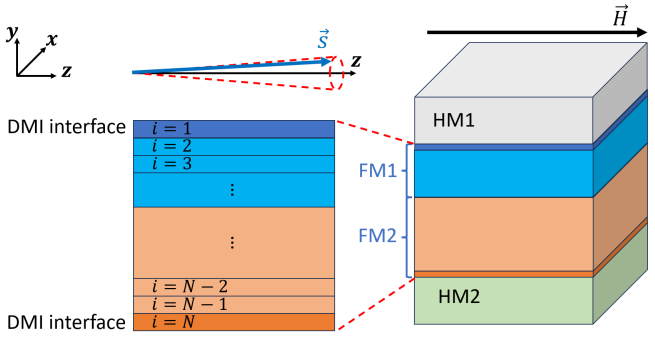

FIG. 1. Example geometry of a multilayer thin film. The film is in the $x - z$ plane. There is a layer of heavy metal (HM) on the top and bottom of the film. There are two layers of different ferromagnetic materials (FM1 and FM2) in the middle of the film. The first DMI interface is the top atomic layer of the first ferromagnetic material (FM1), and another DMI interface is the bottom atomic layer of the second ferromagnetic material (FM2). The externally applied field is in the z direction.

generates nonreciprocal effects. Any in-plane wavevector $\vec{k} = (k_x, k_z)$ may be considered, in general. [31]

In Sec. II the atomic layer method will be described for calculating PSSWs in a magnetic thin film with iDMI. In Sec. III results are presented, first for a single FM material to compare to prior theories. Results for higher-order PSSWs with DMI will be given. Then, PSSWs will be calculated when the magnetic film comprises two FM materials. In Sec. IV, conclusions are provided. In particular, the atomic layer method is adept at calculating magnetization dynamics in any magnetic film with even atomic-level variations in magnetic properties so can be used for calculations beyond those presented here.

II. ATOMIC LAYER METHOD

The calculation method is described in this section. It is similar to in previous works, [28] but with DMI now considered.

We consider a film lying in the x-z plane, with an externally applied field in the $\hat{z}$ direction, as shown in Fig. 1. Since there is translational symmetry in the x-z plane, we aim to write magnetization equations of motion for each atomic layer in the y (film thickness) direction. Material properties can vary layer by layer, meaning that the method outlined can be used to examine films made of one or more materials. The atomic layers are numbered with $i = 1$ being the top magnetic layer, and $i = N$ being the bottom. We consider interfacial DMI which acts only on the top and/or bottom atomic layer.

The total energy density (without the DMI contribu-

tion) is

$$U = -\sum_{<i,j>} \frac{2A_{i,j}}{a^2}\vec{S}_i \cdot \vec{S}_j - \mu_0 \vec{H} \cdot \sum_i \vec{S}_i M_i - \frac{\mu_0}{2}\sum_i M_i^2 \left(S_i^y\right)^2 - \sum_i K_i \left(S_i^y\right)^2 . \quad (1)$$

The first term is the exchange energy density, with $A_{i,j}$ the exchange stiffness between nearest neighbour spins $\vec{S}_i$ and $\vec{S}_j$, at sites denoted i and j, respectively. The $\vec{S}_i$ are unit vectors in the direction of the local magnetization, i.e. $\vec{S}_i = \vec{M}_i/|M_i|$. The sum is over all nearest neighbour pairs and a is the atomic spacing between spins. The second term in Eq. (1) is the Zeeman energy, due to the application of a magnetic field $\vec{H} = H\hat{z}$. M_i is the saturation magnetization associated with spin S_i, which can change through the thin thickness (y direction). The sum is over all sites i. The third term in Eq. (1) is the demagnetizing energy in the thin film approximation. We note that dipolar fields can be treated more rigorously, [30] however, this approximation does a reasonable job of predicting spin wave frequencies. [31, 32] Magnetocrystalline anisotropy and surface anisotropies are represented in the final term of Eq. (1), with K_i an easy-axis anisotropy strength along y in this case. Anisotropy is ignored for now, with the demagnetizing effects assumed to be dominant. [34, 35]

The iDMI energy density was excluded from Eq. (1) as it only occurs on the top and/or bottom atomic layer of the magnetic stack. If l and m denote neighbouring sites within the top (bottom) atomic layer of the film, then the DMI energy is written as a sum over all such pairs, namely

$$U_{\mathrm{DMI}} = \sum_{<l,m>} \frac{\vec{D}_{l,m}}{a^3} \cdot \left(\vec{S}_l \times \vec{S}_m\right), \quad (2)$$

where $\vec{D}_{l,m}$ is the DMI vector for a particular spin pair l and m, with units of Joules. Note that the DMI vector can be expressed as a surface energy density via $D_s = D_{l,m}/a$ with units of J/m, or as the atomic DMI value $D_{\mathrm{at}} = D_{l,m}/a^2$ with units of J/m^2. [1] Furthermore, the *effective* layer-averaged DMI that is commonly used in micromagnetics scales inversely with thickness since here DMI is an interface effect. The effective micromagnetic iDMI constant is given by

$$D_{\mathrm{eff}} = \frac{D_{l,m}}{aL} = \frac{D_{\mathrm{at}}}{N}, \quad (3)$$

where L is the thickness of the film and $D_{\mathrm{eff}} \to D_{\mathrm{at}}$ as the thickness approaches a single atomic layer ($L \to a$ or $N \to 1$). The DMI vector's direction in Eq. (2) is orthogonal to both the symmetry-breaking y direction and also to the distance vector connecting site l to site m. [1, 22]

The magnetic equation of motion for site i can be written in terms of a functional derivative of the energy density, namely

$$\frac{\partial \vec{S}_i}{\partial t} = |\gamma|\, \vec{S}_i \times \left(\frac{1}{M_i}\right)\frac{\delta U}{\delta \vec{S}_i}, \quad (4)$$

where μ_0 is the permeability of free space, γ is the gyromagnetic ratio and M_i is the saturation magnetization at atomic layer i.

Eq. (4) can be linearized by assuming the magnetization is saturated in the $\hat{z}$ direction. The magnetization of site i has two dynamic components in the $\hat{x}$ and $\hat{y}$ direction with small amplitudes ($s_i^x, s_i^y \ll S_z \sim 1$). The unit vector magnetization $\vec{S}_i$ can be approximated as

$$\vec{S}_i\left(\vec{r}_p, t\right) \sim \left(s_i^x e^{i\left(\vec{k}\cdot\vec{r}_i - \omega t\right)}, s_i^y e^{i\left(\vec{k}\cdot\vec{r}_i - \omega t\right)}, 1\right), \quad (5)$$

where $\vec{r}_i$ is the position vector of $\vec{S}_i$, $\vec{k} = (k_x, k_z)$ is the in-plane spin wavevector, and ω is the angular frequency of the spin wave. Two linear equations – for amplitudes s_i^x and s_i^y – in each atomic layer i are obtained by substituting Eqs. (5) and (1) into the magnetization equation of motion (Eq. (4)). The linearized equations are

$$\begin{aligned} -\frac{i\omega}{|\gamma|}\begin{bmatrix} s_i^x \\ s_i^y \end{bmatrix} &= \mu_0 H \begin{bmatrix} s_i^y \\ -s_i^x \end{bmatrix} + \mu_0 M_i \begin{bmatrix} s_i^y \\ 0 \end{bmatrix} \\ &+ \frac{2A_{i,i-1}}{a^2 M_i}\begin{bmatrix} s_i^y - s_{i-1}^y \\ -s_i^x + s_{i-1}^x \end{bmatrix} \\ &+ \frac{2A_{i,i+1}}{a^2 M_i}\begin{bmatrix} s_i^y - s_{i+1}^y \\ -s_i^x + s_{i+1}^x \end{bmatrix} \\ &+ \frac{2A_{i,i}}{a^2 M_i}\left[4 - 2\cos\left(ak_x\right) - 2\cos\left(ak_z\right)\right]\begin{bmatrix} s_i^y \\ -s_i^x \end{bmatrix} \\ &\pm \frac{i2D_{\mathrm{at}}}{aM_i}\delta_{i,1}\sin\left(ak_x\right)\begin{bmatrix} s_i^x \\ s_i^y \end{bmatrix}. \end{aligned} \quad (6)$$

Here, the exchange stiffness between atoms within an atomic layer i is denoted $A_{i,i}$. The exchange stiffness between layer i and nearest neighbours located below (above) it is $A_{i,i+1}$ ($A_{i,i-1}$). The final term in Eq. (6) is the DMI term, with the Kronecker delta $\delta_{i,1}$ ensuring that it only appears for the top layer. Alternately, there could be DMI on the bottom layer N. The atomic DMI constant defined at the interface layer, D_{at}, is used with units of J/m^2.

If there are N atomic layers in the thin film with thickness $L = Na$, then there are $2N$ linear equations. These equations form a spin wave matrix with dimension $2N \times 2N$. The eigenvalues of the matrix are allowed angular frequencies ω and the eigenvectors are the amplitudes $\{s_i^x, s_i^y\}$ of the PSSWs through the film thickness. The lowest eigenfrequency corresponds to the (quasi-)uniform thickness mode ($n = 0$), and higher frequencies correspond to PSSWs with more nodes ($n = 1, 2, \ldots$). Matrix solvers in numerical packages such as numpy or *Mathematica* can be used to find the spin wave modes and frequencies, for a range of in-plane propagation wave vectors $\vec{k} = (k_x, k_z)$, although $\vec{k} = (k_x, 0)$ is primarily considered here.

III. RESULTS

The results are split into two sections. First, in Sec. III A, results for spin waves in a single FM material are given in order to validate the method and to point out differences from previous theories. Second, in Sec. III B, some results are shown for a bilayer comprised of two magnetic materials.

A. One FM material

For a single ferromagnetic material forming a film, an analytic expression for the spin wave dispersion exists. It assumes that the magnetization precession is uniform through the film thickness. It is given by Moon *et al.* [22] and by Kostylev [26] and in our notation plus in the long-wavelength limit is given by

$$\frac{\omega}{|\gamma|} = \sqrt{\left(B + B_{\rm ex}a^2k^2\right)\left(B + \mu_0 M + B_{\rm ex}a^2k^2\right)} + B_{\rm D}ak_x, \tag{7}$$

where the effective magnetic fields are $B = \mu_0 H$, $B_{\rm ex} = 2A/(a^2M)$, $B_{\rm D} = 2D_{\rm eff}/(aM)$ and $k^2 = k_x^2 + k_z^2$. Note that in Ref. [22], the full dipolar contribution is included in the dispersion relation but Eq. (7) is in the long-wavelength, thin film limit.

In Fig. 2, the dispersion relation for the quasi-uniform mode, calculated using the numerical, atomic layer method detailed in Sec. II, is shown (circles and diamonds) compared with the analytic expression of Moon *et al.* (Eq. (7) above, lines). The parameters chosen are based on NiFe (Permalloy) and taken from Ref. [26]. Namely, the applied field $B = 30$ mT (300 Oe), the saturation magnetization $\mu_0 M = 1.05$ T, exchange stiffness $A = 1.355 \times 10^{-11}$ J/m, and gyromagnetic ratio $\gamma = 176$ rad·Hz/T (28 GHz/T). There are $N = 4$ atomic layers with atomic spacing $a = 0.248$ nm, giving a total thickness $L \sim 1$ nm. The interfacial atomic DMI constant $D_{\rm at} = 4.2$ mJ/m^2 acts at the top layer only, which corresponds to an effective DMI used in the analytic expression of $D_{\rm eff} = D_{\rm at}/N = 1.05$ mJ/m^2. Here, $k_z = 0$ and k_x is varied, as it is propagation in the x direction that is influenced by the interfacial DMI.

In Fig. 2, one sees a symmetric dispersion relation when $D_{\rm at} = 0$ for reference (black diamonds), and a well-known nonreciprocal or shifted dispersion curve when DMI is present (red circles). Note that the analytic expression and the numerical results match to within 0.15% for these parameters, as long as one assumes that $D_{\rm eff} = D_{\rm at}/N$, where $D_{\rm eff}$ is used in the analytical equation and $D_{\rm at}$ is used at the interface atomic layer ($i = 1$) in the numerical approach.

This match supports the validity of the atomic layer method to calculate PSSWs in thin films. Unlike the analytic Eq. (7), the atomic layer method is able to calculate the dispersion for higher order PSSWs, not just the uniform ($n = 0$) mode which was plotted in Fig. 2.

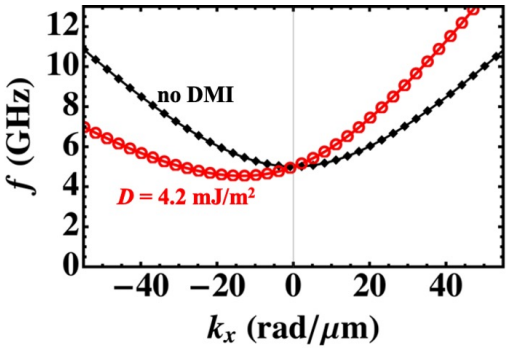

FIG. 2. The dispersion relation for the quasi-uniform thickness mode without DMI (black diamonds) and with $D_{\rm at} = 4.2$ mJ/m^2 (red circles) applied to the top layer only, calculated using the atomic layer method. The lines under the data points show corresponding results of Ref. [22] (Eq. (7)), with $D_{\rm eff} = D_{\rm at}/4$. The parameters based on four atomic layers of NiFe are given in the main text.

Moreover, the slight discrepancy (less than 0.15%) between the analytic formula and numerical results is due to a relaxation of the assumption that the precession is uniform through the film thickness, which will be discussed more later.

We therefore move to examining the frequencies of higher order thickness modes or PSSWs in a film made of a single material. These can also be calculated using the continuum model of Kostylev, [26] so we compare our results to those from our version of a continuum model later.

The three panels of Fig. 3 show the dispersion relation for the three lowest-frequency PSSWs in a $N = 16$ atomic layer ($L \sim 4$ nm) NiFe film. All the parameters are the same as those used to generate Fig. 2 and were given in the main text, earlier in this section. Note, however, that the film is now thicker, meaning the effective DMI constant $D_{\rm eff} = D_{\rm at}/N = 0.2635$ mJ/m^2 is four times smaller than for Fig. 2. Fig. 3(a) shows the frequency as a function of in-plane wavevector k_x for the mode that is uniform through the film thickness. The quasi-uniform mode is shown in the schematic to the right of panel (a), with the spin wave having almost constant amplitude as a function of the thickness y direction. Notice that the dispersion curve looks very similar to that shown in Fig. 2, although the characteristic nonreciprocity or shift of the dispersion curve to the left is not as strong since $D_{\rm eff}$ is reduced.

The presence of DMI results in a pinning of the PSSW modes at the top surface, which is imperceptible in Fig. 3. The pinning is different for spin waves depending on the sign of k_x. This was studied in detail by Kostylev, [26] with a full dipole-exchange calculation and for the quasi-uniform mode ($n = 0$). Fig. 4 shows a zoom-in of the spin wave profile at the top surface of the film, for the quasi-uniform mode in the right cartoon of Fig. 3(a). One sees that without DMI, the mode is truly uniform through the film thickness (blue dots), but with DMI and depending

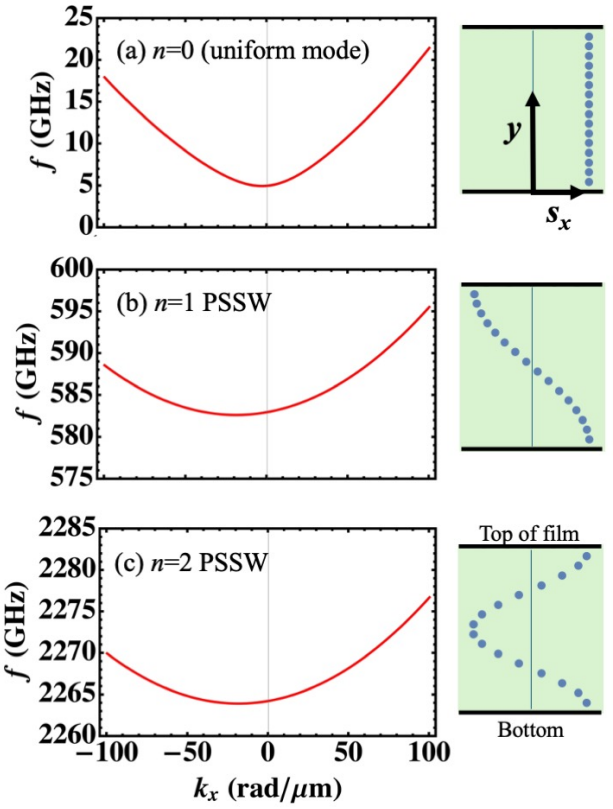

FIG. 3. Dispersion relations for the three lowest-frequency modes in a 16 atomic layer NiFe film with $D_{\rm at} = 4.2$ mJ/m^2 applied at the top surface only. Frequency is plotted versus in-plane wavevector k_x, perpendicular to the saturation magnetization direction. Panel (a) is for the uniform mode, (b) is for the first-exchange mode or $n = 1$ PSSW, and (c) is for the $n = 2$ PSSW. Notice the large difference in frequency range on the vertical axes. To the right of each panel is a schematic of the standing wave through the film's thickness (y direction). The film thickness $L \sim 4$ nm. All other parameters are the same as for Fig. 2 and are given in the main text, based on Ref. [26].

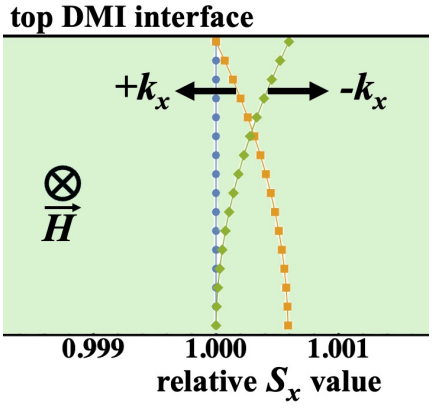

FIG. 4. Zoom in on the quasi-uniform PSSW profile from Fig. 3(a), in order to see the effects of DMI-induced pinning on the top surface. The dots correspond to no DMI (uniform mode profile). The squares and diamonds correspond to $k_x = \pm 20$ rad/μm, respectively. The S_x mode amplitudes are all normalized to a value of one at the top/bottom surface to most clearly illustrate the change in shape.

on the sign of k_x (squares and diamonds), the pinning results in nonuniform precession. For this reason, we refer to the $n = 0$ PSSW as the *quasi*-uniform mode. Notice the horizontal scale in Fig. 4 for the normalized amplitude is very small. However, the introduction of even a tiny curvature in the PSSW profile can have a dramatic result on the frequencies, since the exchange energy density goes as Ak_y^2, with k_y the effective out-of-plane spin wavevector.

Fig. 3(b) and (c) show higher order PSSWs with mode number $n = 1$ (first exchange mode) and $n = 2$ (second exchange mode), respectively. These modes are pictured to the right. There is a very large exchange energy contribution to the frequencies since the wavevector in the thickness direction k_y is large due to standing waves forming within the small thickness $L \sim 4$ nm. Frequencies are on the order of 585 and 2265 GHz, respectively. Notice that for the higher order PSSWs, the DMI has resulted in a larger shift in the dispersion relation as compared to what is observed for the quasi-uniform thickness mode. The reason for this is nontrivial, as the DMI contribution to the spin wave frequency is not as simple for higher order PSSWs as it is under the assumption of uniform motion through the film thickness (Eq. (7)).

To explore PSSW frequency shifts in some detail, we derived an analytic expression for the frequencies of the quasi-uniform mode and the first order PSSW ($n = 0$ and 1). Details of this derivation are in the Appendix, and the final result is Eq. (A.4). One sees that the DMI contributions (inside effective fields $b_\pm$, which scale with $D_{\rm I} \pm D_{\rm II}$, with $D_{\rm I/II}$ the atomic DMI strength at the top/bottom surfaces) multiply by exchange fields (inside B_1 and B_2) meaning that the effect of the DMI on the spin wave frequencies is difficult to predict in a simple way. This result in the Appendix will be discussed more later in this section.

Note that when $k_x = k_z = 0$, the frequency of all modes ($n = 0, 1$ and 2) is unchanged with and without iDMI. This is not the case when there is surface anisotropy, which is known to induce frequency shifts of the FMR modes at $k_x = k_z = 0$. [20]

It is well-studied that increasing the thickness L of a film will decrease the exchange energy and will therefore decrease the frequencies of higher order PSSW. [36, 37] Those frequencies enter the low GHz region. However, this same increase in the film thickness typically leads to a decrease in the effective interfacial DMI constant $D_{\rm eff}$ for a single-phase film, as discussed earlier. Thus, any interesting effects of DMI on the higher order PSSWs are small. A way to circumvent this is to have multiple DMI interfaces within a ferromagnetic film, [38] although it is difficult to make the various layers exchange-coupled. We note that the atomic layer method of spin

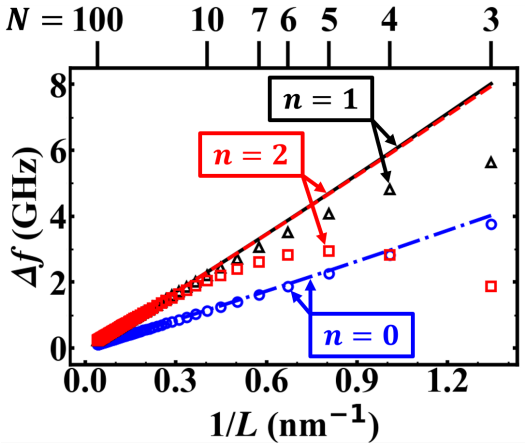

FIG. 5. The nonreciprocity or frequency asymmetry due to DMI (Δf in Eq. (8)) as a function of inverse film thickness $1/L$, for $k_x = 20$ rad/ μm. The film thickness ranges from 24.8 nm ($N = 100$) to 0.74 nm ($N = 3$). Results for the first three PSSWs are shown using the atomic layer method (markers) and using a continuum calculation similar to that in Ref. [26] (lines). Parameters are those of NiFe, as in Figs. 2 and 3, with $D_{\rm at} = 4.2$ mJ/m^2 at the top surface only.

wave calculation detailed here is able to easily model such systems containing many different materials; one simply changes the magnetic parameters in the equation of motion, Eq. (6), for each atomic layer i.

To characterize the size of the nonreciprocity for various PSSWs illustrated in Fig. 3, one can define a frequency asymmetry

$$\Delta f(n, k_x) = f(n, +k_x) - f(n, -k_x). \qquad (8)$$

When there is no DMI, the spin wave asymmetry is zero for all PSSW indices n and for all in-plane wavevector k_x. In Fig. 5 we plot the spin wave asymmetry as a function of inverse film thickness $1/L$ for the $n = 0, 1$ and 2 PSSWs that were shown in Fig. 3, with $k_x = 20$ rad/μm. Once again, parameters are appropriate for NiFe. Along the top of the frame, the corresponding number of atomic layers N is given. This plot is inspired by the second figure in Ref. [26], where only the uniform PSSW ($n = 0$) was plotted. Results of our atomic layer method are shown by the plot markers and results of a continuum calculation based on Ref. [26] are shown by the lines. Note that Ref. [26] uses a much more sophisticated treatment of the dipolar interactions. Here, the continuum model is used with the thin film approximation for the demagnetizing energy included, so as to directly compare to our atomic layer method results.

In Fig. 5, one sees that the uniform mode ($n = 0$) has a frequency asymmetry that scales linearly with inverse thickness. This matches the analytic Eq. (7) where there is a frequency shift that scales with $D_{\rm eff} = D_{\rm at}/N$. The same observation was made in Ref. [26]. It also matches with the more-sophisticated frequency Eq. (A.4) that we analytically derive in the Appendix. The full atomic layer model thus supports the use of an effective DMI constant of this form. The two numerical methods of calculation (markers and lines) match well with each other and with the analytic prediction.

For the higher order PSSWs ($n = 1$ and 2) the two methods of calculation do not match for thinner films. For example, for $N = 4$ atomic layers (inverse thickness $1/L = 1.008$ nm^{-1}) and the second PSSW ($n = 2$), the frequency asymmetry is calculated as 2.82 GHz using the atomic layer model while it is almost 6 GHz using the continuum model. This is perhaps unsurprising because resolving a standing wave with two nodes (see Fig. 3(c) cartoon) using only four atomic layers is very different from drawing the same standing wave on a continuous domain. We are observing a decrease in the exchange energy due to the limited number of atomic sites. Unlike for the uniform mode ($n = 0$), the frequency asymmetry for higher order PSSWs does not strictly scale with inverse thickness, except for the very thickest films with $N > 10$.

Just as was noted for Fig. 3, in Fig. 5 the higher order PSSWs ($n = 1$ and 2, black triangles and red squares) have a larger frequency asymmetry than the quasi-uniform mode (blue circles) for most film thicknesses. This is not the case for the very thinnest films (right of plot) where $n = 2$ has the smallest frequency asymmetry.

For some thin films, there is DMI on the top and bottom interface such as Pt/Co/Pt [39] and Pt/Co/Ir. [40] The DMI contributions can be additive or subtractive, depending on the material combinations or even on the growth order and method. [40] The atomic layer model is able to handle such scenarios. In particular, we comment here on the case of a film with reflection symmetry so that the DMI is equal at each surface, with vector directions opposite. In this case, it is commonly assumed that the two interface contributions cancel and $D_{\rm eff} = 0$. We found that this is not strictly true in calculations using the numerical atomic layer method. The presence of equal DMI on both interfaces leads to frequency shifts in the MHz range. Such a small shift may be difficult to measure in an experiment because any small variation in the DMI strength $D_{\rm at}$ at an interface is likely to lead to a larger effect.

To demonstrate this, Fig. 6 plots the difference in frequency between a system with DMI $f(D)$ and one without $f(0)$, as a function of in-plane wavevector k_x. There are 16 atomic layers and all magnetic parameters are the same as in previous figures. In this case, the atomic DMI strength is $D_{\rm at} = 9.0$ mJ/m^2, which is stronger than for previous results in this article but is theoretically possible. [41] The top and bottom interfaces are assumed identical so that the $D_{\rm eff} = 0$. However, the frequency difference in Fig. 6 is non-zero. For wavevectors around 20 rad/μm, which are accessible in Brillouin Light Scattering (BLS) experiments, the frequency difference due to DMI is around 0.05 GHz, which is perhaps at the limit of BLS resolution but measurable with propagating spin

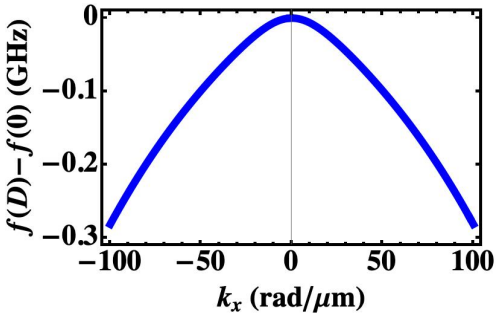

FIG. 6. The difference in the quasi-uniform mode frequency with DMI $f(D)$ and without DMI $f(0)$ as a function of in-plane wavenumber k_x, for a thin film with two identical interfaces. There are 16 atomic layers and $D = 9.0$ mJ/m^2 on the top and bottom surface. Other magnetic parameters are the same as those used throughout this section. The atomic layer method is used to get this result. Using Eq. (7), one would expect the frequency difference to be zero.

wave spectroscopy, with resolution quoted of 1 Hz. [42]

To explain the small frequency shift when DMI is equal at the top and bottom interface, we developed an analytic expression for the frequency of PSSWs in a magnetic film split into two macrospin layers. Details are in the Appendix. This is the first step in moving beyond a theory that assumes uniform magnetization through a film thickness. The expression is written in the Appendix as Eq. (A.4). It depends on an effective DMI field on the top $b_{\rm I}$ and on the bottom $b_{\rm II}$, with opposite DMI vector directions assumed. If the DMI on the bottom is made zero, then Eq. (A.4) collapses to be similar to the dispersion relation by Moon *et al.* (Eq. (7)), in the long wavelength limit. However, consider the case where $b_{\rm I} = b_{\rm II}$. Then, although the leading term linear in $(b_{\rm I} - b_{\rm II})$ vanishes in Eq. (A.4), smaller cross terms involving $(b_{\rm I} + b_{\rm II})$ remain. It is these nonlinear cross terms which result in a tiny change in the PSSW frequencies, even when $D_{\rm eff} \to 0$.

Recall in Fig. 2 that there was less than 0.15% difference between our calculation for the quasi-uniform mode frequency compared to the analytic expression Eq. (7). This fact can be explained by the small, nonlinear dependence of the PSSW frequencies on the DMI strength (see Eq. (A.4)), which is not captured when the precession is assumed perfectly uniform through the film thickness.

Recently, Yang *et al.* developed an analytic expression for the frequency of two FM layers with equal heavy metal capping on the top and bottom interfaces, [33] but for the case where saturation magnetization is in the out-of-plane y direction instead of in-plane direction as considered here. The strengths of iDMI on the top and bottom of the ferromagnetic layers were taken to be equal $(b_{\rm I} = b_{\rm II})$. A similar reduction of spin wave frequencies with iDMI – apparent in our Fig. 6 – was also found in their results, which were confirmed by MuMax3 simulation.

We have focused on the case of $b_{\rm I} = b_{\rm II}$ here, although both the atomic layer method and analytic expression in the Appendix are far more general. This is because the fact iDMI shifts the PSSW frequencies is unexpected when $b_{\rm I} = b_{\rm II}$ or alternately $D_{\rm eff} = 0$. However, it is difficult to make a multilayer with exactly $b_{\rm I} = b_{\rm II}$. Any small asymmetry $(b_{\rm I} \neq b_{\rm II})$ causes Fig. 6 to become asymmetric. In this way, one may be able to probe the relative contributions of iDMI at the top and bottom interfaces, through a mapping of frequency shifts $f(D) - f(0)$ across a broad range of wavenumbers $\vec{k}$.

B. Two FM material

In this subsection, results for a bilayer magnetic film are given. This example is chosen because it represents a geometry for which a continuum theory for PSSWs [26] cannot easily be used to calculate frequencies and modes. In this way, the atomic layer method shows great utility. This example is also chosen to explore how magnetic parameters affect frequency shifts due to DMI.

An example of a bilayer structure shown in Fig. 1 is Ir/Fe/Co/Pt. [38, 43] The DMI vectors at the Ir/Fe and Co/Pt interfaces are in the same direction. This gives an additive enhancement of DMI strength in the thin film system. The magnetic parameters chosen for this example are as follows. For the iron layer, the saturation magnetisation $M = 1750$ kA/m, [44] the exchange stiffness $A = 18.8$ pJ/m, [45] the gyromagnetic ratio $\gamma = 29.0$ GHz/T, [46] and the atomic spacing $a = 0.2866$ nm. [45] For the Cobalt layer, the saturation magnetisation $M = 1450$ kA/m, [44] the exchange stiffness $A = 32.5$ pJ/m, [45] the gyromagnetic ratio $\gamma = 31.2$ GHz/T, [47] and the atomic spacing $a = 0.2506$ nm. [45] The exchange stiffness at the ferromagnetic interface Fe/Co is assumed to be $A = 27$ pJ/m. [48] The externally applied field $B = 30$ mT (300 Oe). There are $N = 20$ atomic layers in total, which consist of 10 atomic layers for iron and 10 atomic layers for cobalt. The interfacial atomic DMI constant is $D_{\rm at} = D_{\rm I} = 3.9$ mJ/m^2 at the Ir/Fe interface [49], and $D_{\rm at} = D_{\rm II} = -1.5$ mJ/m^2 at the Co/Pt interface. [11]

Fig. 7(a) shows the spin wave frequency of the quasi-uniform mode $(n = 0)$ as a function of in-plane wavenumber k_x, for the Ir/Fe/Co/Pt stack. Panels (b) and (c) shows the dispersion of the two higher order modes $(n = 1$ and 2), respectively. The dispersion for a FM bilayer is similar in shape to that of a single FM film (compare these plots to Fig. 3). However, the higher-order PSSW profiles – shown as cartoons to the right of each dispersion plot – are different. While for a single FM film the modes were symmetric about the center of the film, now the modes are shifted. In particular, the modes have a shorter wavelength in the iron (top layer) compared to the cobalt (bottom layer) because iron has a softer exchange stiffness. This behavior has been studied before in magnetic multilayers without DMI [30, 31] and these results show that it is possible to further fine tune the spin wave behavior using DMI.

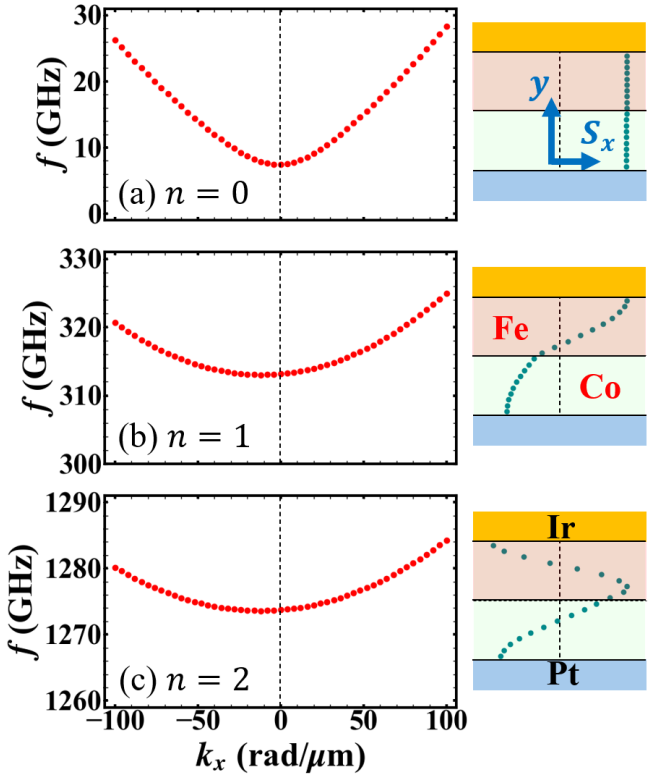

FIG. 7. Dispersion relation for the three lowest-frequency modes in a Ir/Fe/Co/Pt stack with $D_{\rm at} = 3.9$ mJ/m^2 at the Ir/Fe surface and $D_{\rm at} = -1.5$ mJ/m^2 at the Co/Pt surface. There are 10 atomic layers of iron and 10 atomic layer of cobalt. Panel (a) is for the quasi-uniform mode ($n = 0$), (b) is for the first-exchange mode ($n = 1$), and (c) is for the second-exchange mode ($n = 2$). Notice the frequency range is different for the three modes on the vertical axes. To the right of each panel is a schematic of the PSSW profile through the film's thickness (y direction). The magnetic parameters are given in the main text.

We now show that, surprisingly, frequency shifts due to DMI do not just depend on the DMI strength. At the start of Sec. III A, the effective DMI field when DMI was at one interface was given by $B_D = (2D_{\rm eff})/(aM) = (2D_{\rm at})/(aMN)$. That is, the effective DMI field depends on the DMI strength at a single atomic interface $D_{\rm at}$, on the film thickness $L = aN$, and on the saturation magnetization M. In Eq. (7) – derived for uniform precession through the film thickness – the DMI effective field is seen to affect the uniform mode's frequency in isolation from other magnetic contributions. We have already discussed that when the assumption of uniform precession is removed – even for the quasi-uniform mode – then the dynamics become more complicated. Eq. (A.4) in the Appendix is a first approximation to show this. One sees that exchange fields multiply by effective DMI fields so that the effect of DMI on PSSW frequencies is difficult to predict. In short, the frequency shift due to DMI should now depend on other magnetic parameters such as A and H, which is not expected using the much-used Eq. (7).

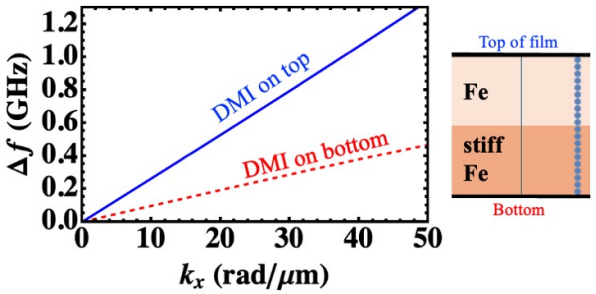

FIG. 8. The frequency asymmetry (or nonreciprocity, Eq. (8)) as a function of in-plane wavenumber amplitude k_x for a bilayer comprising 20 atomic layers. Here, magnetic parameters are that of iron, with the top 10 atomic layers having regular exchange stiffness, and the bottom 10 layers having exchange that is artificially four times larger. Results for the quasi-uniform ($n = 0$) mode are shown (see schematic to the right). When an atomic DMI strength of 3.9 mJ/m^2 is acting on the top surface (blue, solid line) then the frequency asymmetry is over twice as large as if it were acting on the bottom surface (red, dashed line).

For a magnetic bilayer, we can test this hypothesis since the exchange stiffness A is different for the two FM materials. Consider an artificial bilayer with $N = 20$ where all the magnetic parameters are that of iron (see the start of this subsection for values) but the exchange is four times as large on the bottom half than the top. This situation is shown by the schematic to the right in Fig. 8. If the DMI of 3.9 mJ/m^2 is on the *top* surface then it results in a different frequency asymmetry (nonreciprocity, Eq. (8)) than if it were on the bottom surface, even though $D_{\rm eff}$ is the *same* for both cases. In Fig. 8 the frequency asymmetry for the $n = 0$ mode is plotted as a function of the in-plane wavenumber amplitude k_x. When the DMI is on the top (blue, solid line), it has a larger effect on the frequencies than if the same DMI strength were on the bottom (red, dashed line). This is because the stiffer iron layer on the bottom is less affected by DMI pinning.

With this example, one sees that the DMI and exchange contributions to the frequency are intimately coupled, as may be expected from our analytic approximation Eq. (A.4). This is the case even for the quasi-uniform mode. Physically, the interfacial DMI pinning affects the PSSW profiles differently at the top and bottom surface because the profiles are not symmetric about the center of the film. Any small shift in k_y in turn affects the exchange energy and therefore the PSSW frequency.

IV. CONCLUSION

In this article, we have examined PSSW frequencies and mode profiles in thin magnetic films with interfacial DMI. An "atomic layer method" that is well-used in the literature for other spin wave problems [28, 29] is applied here to DMI systems. The method has the advantage

of being able to treat thin films with non-uniformities at the atomic scale. For example, multilayered films can be treated, or materials with gradient magnetization or exchange. [25, 50] This provides an advantage compared to a "continuum model" by Kostylev [26], which is best suited for uniform magnetic properties throughout a film. Ref. [26] was the pioneering work to examine DMI pinning of PSSWs, focusing on the uniform mode. Another advantage of the atomic layer method is that it is quasi-one-dimensional, meaning it is less computationally demanding than using micromagnetics to calculate for in-plane propagating PSSWs.

In this article, the atomic layer method is implemented with the thin film approximation used for the demagnetizing energy. This has been shown to be appropriate in the long-wavelength limit, [31] but should be relaxed in future work to properly calculate dipole-exchange spin waves.

We show that PSSWs of different order $n = 0, 1, 2, \ldots$ have a different value for the frequency asymmetry or nonreciprocity Δf due to DMI. For some films, the $n = 2$ mode has a larger Δf than the quasi-uniform $n = 0$ mode, while for other films the opposite is true (see Fig. 5). This behavior is difficult to predict because the spin wave frequencies depend in a nonlinear way on the effective DMI field.

The nonlinear dependence of the PSSW frequencies on the DMI field is not expected using the much-used frequency expression Eq. (7), which is derived assuming uniform PSSW amplitude through the thin film thickness. In reality, even the $n = 0$ PSSW has some nonuniformity, and this leads to a weak coupling between the exchange field and the DMI field. This is seen in our studies in multiple instances. First, a less than 0.15% change in the predicted quasi-uniform PSSW frequency for a single magnetic film is calculated, compared to Eq. (7). Second, we show that DMI affects the PSSW frequencies on the MHz scale, even when the DMI at a top and bottom interface appear to cancel each other out. Third, we demonstrate using an artificial bilayer that the exchange stiffness near a surface affects the nonreciprocity Δf resulting from iDMI.

Although the frequency results are all calculated using the atomic layer model, an analytic approximation is provided in the Appendix based on two macrospin slabs that experience different DMI values at the top and bottom interfaces. The analytic approximation – given in Eq. (A.4) – also shows the nonlinear dependence of the frequencies on the effective DMI field, plus the coupling of the DMI field to other effective fields like that due to exchange. Note that recently an analytic result was derived by Yang *et al.* [33], but for a different geometry than that considered here, and also limiting the DMI strength to be equal and opposite on the top and bottom interfaces. Nevertheless, they saw a similar reduction in spin wave frequencies when $D_{\text{eff}} = 0$.

We have provided results based on experimental values for NiFe and Ir/Fe/Co/Pt. In the future, the atomic layer method can be used to find PSSW frequencies and mode profiles in a wide range of stacks containing more than one material, or material gradients, where analytic theories break down. This is especially important as more multilayered DMI materials are developed for applications in spintronics. [51]

Appendix: Analytic approximation for a film split into two slabs

In this Appendix, an analytic expression for the frequencies of the quasi-uniform and first exchange PSSWs ($n = 0$ and 1) is provided. The analytic estimate provides insight into how DMI affects spin wave frequencies. It goes beyond the estimate of Eq. (7), which assumes uniform magnetization precession through the film thickness.

Consider a magnetic film of thickness $L = Na$ with uniform magnetic properties. N is the number of atomic layers. Both the top and bottom surfaces may have interfacial DMI, with strength given by $D_{\text{eff}}^{\text{I}}$ on top and $D_{\text{eff}}^{\text{II}}$ on bottom. If both the top and bottom interfaces are identical (say NiFe with Pt on both sides), then $D_{\text{eff}}^{\text{I}} = D_{\text{eff}}^{\text{II}}$, however the DMI vectors point in opposite directions because the magnetic film normal vectors are in opposite directions. In this scenario, the iDMI is subtractive and the total effective DMI strength $D_{\text{eff}} = 0$. We assume that the DMI vectors are in opposite directions in what follows for simplicity, but this assumption can be generalized.

The film is artificially split into two slabs I and II, with representative macrospins in each one. This scenario is shown in Fig. 9. The two macrospins, $\vec{S}_{\text{I}}$ and $\vec{S}_{\text{II}}$, can precess with different phases. By splitting the film into two slabs, we have the minimum model that goes beyond the assumption of uniform motion through the film thickness. Having only two macrospins – rather than defining spins in every atomic spin layer – allows for an approximate, analytic expression for the spin wave frequencies to be found.

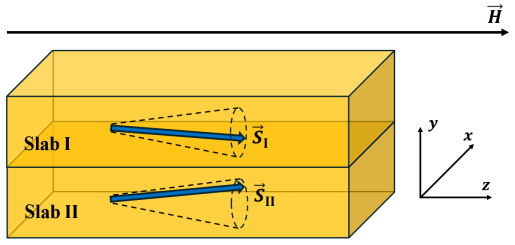

FIG. 9. The geometry of the thin film split into two equal slabs I and II. The film is in the x-z plane. $\vec{S}_{\text{I}}$ is the macrospin of slab I, and $\vec{S}_{\text{II}}$ is the macrospin of slab II. There may be DMI interfaces on the top and bottom of the film. The external applied field saturates the magnetization in the z direction.

As described in Sec. II, each spin is governed by an equation of motion Eq. (4). In turn, these equations are determined by the magnetic energy density of the film. For the two slabs, we re-write the energy density of Eq. (1) in terms of macrospins $\vec{S}_{\rm I}$ and $\vec{S}_{\rm II}$. The result is

$$\begin{aligned} U' = &-\sum_i \frac{2A}{a^2(N/2)^2}\vec{S}_{{\rm I},i}\cdot\vec{S}_{{\rm II},i} - \sum_{\langle i,j\rangle}\frac{2A}{a^2}\vec{S}_{{\rm I},i}\cdot\vec{S}_{{\rm I},j} \\ &-\sum_{\langle i,j\rangle}\frac{2A}{a^2}\vec{S}_{{\rm II},i}\cdot\vec{S}_{{\rm II},j} - \mu_0 M\vec{H}\cdot\sum_i\left(\vec{S}_{{\rm I},i}+\vec{S}_{{\rm II},i}\right) \\ &+\frac{\mu_0}{2}M^2\sum_i\left(S^2_{{\rm I},i,y}+S^2_{{\rm II},i,y}\right) \\ &+\sum_{\langle i,j\rangle}\frac{D_{\rm I}}{a(N/2)}\hat{z}\cdot\left(\vec{S}_{{\rm I},i}\times\vec{S}_{{\rm I},j}\right) \\ &-\sum_{\langle i,j\rangle}\frac{D_{\rm II}}{a(N/2)}\hat{z}\cdot\left(\vec{S}_{{\rm II},i}\times\vec{S}_{{\rm II},j}\right) \end{aligned} \tag{A.1}$$

Here, the first term on the left-hand-side describes the exchange energy between the top slab and the bottom slab. The index i counts over all atomic sites in the x-z plane, so that spin waves can propagate in these directions. Notice that the effective exchange constant between the two macrospins is reduced by a factor of $(N/2)^2$ compared to nearest-neighbour spin pairs, where N is the number of atomic layers within the film thickness.

The second term in Eq. (A.1) describes the exchange energy within the top slab. The notation $\langle i,j\rangle$ denotes a sum over all nearest neighbour atomic pairs within the x-z plane. Similarly, the third term denotes the exchange energy within the bottom slab.

The fourth term in Eq. (A.1) is the Zeeman energy, summed over all in-plane sites i. The fifth term is the approximate thin film demagnetizing energy.

Finally, the last two terms are the DMI contributions for the top and bottom slabs, respectively. Since the magnetization is saturated in the z direction, it is only spin wave propagation in the x direction that is affected by iDMI. Here, $D_{\rm I}$ is the interface DMI at the top layer and the effective DMI for the slab is $D^{\rm I}_{\rm eff} = D_{\rm I}/(N/2)$, since the DMI is averaged over half the thickness or $N/2$ atomic layers. A similar expression exists for the bottom interface with $D_{\rm II}$, except the sign is reversed in Eq. (A.1).

As in Sec. II where the atomic layer method was described, with the two slab model one substitutes the energy density into the equation of motion (4), linearizes by assuming saturation in the z direction (see Eq. (5)), and then arrives at a matrix equation of the form

$$\hat{X}\cdot\begin{pmatrix} S_{{\rm I},x} \\ S_{{\rm I},y} \\ S_{{\rm II},x} \\ S_{{\rm II},y}\end{pmatrix} = 0, \tag{A.2}$$

where $\hat{X}$ is a matrix given by

$$\hat{X} = \begin{pmatrix} -i\frac{\omega}{|\gamma|} - ib_{\rm I} & B_2 & 0 & -B^Y_{ex} \\ B_1 & -i\frac{\omega}{|\gamma|} - ib_{\rm I} & B^Y_{ex} & 0 \\ 0 & -B^Y_{ex} & -i\frac{\omega}{|\gamma|} + ib_{\rm II} & B_2 \\ B^Y_{ex} & 0 & B_1 & -i\frac{\omega}{|\gamma|} + ib_{\rm II}\end{pmatrix}. \tag{A.3}$$

Various shorthand notations are used here for effective magnetic fields, including

$$\begin{aligned} b_{\rm I} &= \frac{D_{\rm I}}{a(N/2)M}2\sin(k_x a) \\ b_{\rm II} &= \frac{D_{\rm II}}{a(N/2)M}2\sin(k_x a) \\ B_{ex} &= \frac{2A}{a^2 M} \\ B^Y_{ex} &= \frac{B_{ex}}{(N/2)^2} \\ B_1 &= B_{ex}\left[4 - 2\cos(k_x a) - 2\cos(k_z a)\right] \\ &\quad + B^Y_{ex} + \mu_0 H \\ B_2 &= B_1 + \mu_0 M. \end{aligned}$$

The solution to Eq. (A.2) yields four frequencies. Of these, two are negative and unphysical. The two remaining frequencies represent estimates for the quasi-uniform mode and first exchange mode frequencies. They are given by

$$\frac{\omega}{|\gamma|} = b_- + \sqrt{\begin{array}{l} b_+^2 + (B^Y_{ex})^2 + B_1 B_2 \\ \mp\sqrt{4B_1B_2b_+^2 + (B_1+B_2)^2(B^Y_{ex})^2}\end{array}} \tag{A.4}$$

where the top and bottom effective DMI fields are combined according to

$$b_\pm = \frac{1}{2}\left(b_{\rm I} \pm b_{\rm II}\right). \tag{A.5}$$

In the limit that the DMI vanishes and the two slabs I and II are decoupled ($B^Y_{ex}\to 0$), then Eq. (A.4) recovers the correct spin-wave frequency in the long-wavelength limit

$$\begin{aligned} \frac{\omega}{|\gamma|} &= \sqrt{B_1 B_2} \\ &\sim \sqrt{\left(\frac{2A}{M}k^2 + \mu_0 H\right)\left(\frac{2A}{M}k^2 + \mu_0 H + \mu_0 M\right)}. \end{aligned} \tag{A.6}$$

Notice the $\mp$ sign in the frequency expression Eq. (A.4); the negative solution corresponds to the uniform mode frequency and the positive solution is that of the first exchange mode. We have verified that the uniform mode expression matches extremely well with full numerical calculations using the atomic layer method, for films of any thickness. However, the first exchange mode frequency is approximated poorly because the full exchange energy of a PSSW cannot be captured by a model that

uses just two values to represent the magnetization variation through the film thickness. Even though there is quantitative disagreement for the first exchange mode, Eq. (A.4) reveals qualitative information on the spin wave frequency's dependence on the DMI strength.

The first term on the right-hand-side of Eq. (A.4) (b_-) is outside the square root and scales with the DMI strength difference ($D_{\rm I} - D_{\rm II}$). It is the *same term* seen in Eq. (7) by Moon *et. al*, [22] derived for a film with uniform magnetization through the film thickness. Namely, we have

$$b_- = \frac{1}{2}\left(D_{\rm I} - D_{\rm II}\right)\frac{2\sin(k_x a)}{a(N/2)M} \tag{A.7}$$

which simplifies to

$$b_- = \frac{2D_{\rm at}}{aNM}\sin(k_x a) \sim \frac{2D_{\rm eff}}{M}k_x, \tag{A.8}$$

in the limit that there is only DMI on the top interface and in the long-wavelength limit ($\sin(k_x a) \sim k_x a$). On the other hand, this term b_- will completely vanish if the top and bottom interfaces of a film are identical. In experiment, this complete cancellation may be difficult to achieve due to any growth asymmetry.

However, unlike the simpler expression in Eq. (7), in our derived Eq. (A.4) one sees that there is also a nonlinear dependence of the frequency on the DMI strength through b_+, which scales with $(D_{\rm I} + D_{\rm II})$. The nonlinear dependence is weak, but points to the possibility of DMI affecting spin wave frequencies even when the top and bottom interface contributions would apparently cancel out in the much-used Eq. (7). This is discussed in the main text.

Yang *et al.* also found that the DMI provides a weak and symmetric contribution to the dispersion relation when the iDMI values are equal and opposite on the top and bottom interfaces ($b_- = 0$). [33] We have a different expression compared to Yang *et al.* because they consider the case where the magnetization is saturated out-of-plane (forward volume geometry), whereas we consider the in-plane case (surface wave geometry). Comparing Eq. (A.4) to their analytic expression, the out-of-plane geometry does not result in a nonlinear dependence of the frequency on b_+, as we find for in-plane saturation.

[1] R. E. Camley and K. L. Livesey, Consequences of the Dzyaloshinskii-Moriya interaction, Surf. Sci. Rep. **78**, 100605 (2023).

[2] T. Moriya, Anisotropic superexchange interaction and weak ferromagnetism, Phys. Rev. **120**, 91 (1960).

[3] I. Dzyaloshinsky, A thermodynamic theory of "weak" ferromagnetism of antiferromagnetics, J. Phys. Chem. Solids **4**, 241 (1958).

[4] A. Crépieux and C. Lacroix, Dzyaloshinsky-Moriya interactions induced by symmetry breaking at a surface, J. Magn. Magn. Mater. **182**, 341 (1998).

[5] E. Y. Vedmedenko, L. Udvardi, P. Weinberger, and R. Wiesendanger, Chiral magnetic ordering in two-dimensional ferromagnets with competing Dzyaloshinsky-Moriya interactions, Phys. Rev. B **75**, 104431 (2007).

[6] M. Heide, G. Bihlmayer, and S. Blügel, Dzyaloshinskii-Moriya interaction accounting for the orientation of magnetic domains in ultrathin films: Fe/W (110), Phys. Rev. B **78**, 140403 (2008).

[7] K. Zakeri, Y. Zhang, J. Prokop, T.-H. Chuang, N. Sakr, W.-X. Tang, and J. Kirschner, Asymmetric spin-wave dispersion on Fe (110): Direct Evidence of the Dzyaloshinskii-Moriya Interaction, Phys. Rev. Lett. **104**, 137203 (2010).

[8] Q. Zhang, J. Liang, K. Bi, L. Zhao, H. Bai, Q. Cui, H.-A. Zhou, H. Bai, H. Feng, W. Song, G. Chai, O. Gladii, H. Schultheiss, T. Zhu, J. Zhange, Y. Peng, H. Yang, and W. Jiang, Quantifying the Dzyaloshinskii-Moriya interaction induced by the bulk magnetic asymmetry, Phys. Rev. Lett. **128**, 167202 (2022).

[9] R. Magaraggia, K. Kennewell, M. Kostylev, R. L. Stamps, M. Ali, D. Greig, B. J. Hickey, and C. H. Marrows, Exchange anisotropy pinning of a standing spin-wave mode, Phys. Rev. B **83**, 054405 (2011).

[10] R. E. Camley, T. S. Rahman, and D. L. Mills, Theory of light scattering by the spin-wave excitations of thin ferromagnetic films, Phys. Rev. B **23**, 1226 (1981).

[11] M. Kuepferling, A. Casiraghi, G. Soares, G. Durin, F. Garcia-Sanchez, L. Chen, C. H. Back, C. H. Marrows, S. Tacchi, and G. Carlotti, Measuring interfacial Dzyaloshinskii-Moriya interaction in ultrathin magnetic films, Rev. Mod. Phys. **95**, 015003 (2023).

[12] T. Schneider, A. A. Serga, B. Leven, B. Hillebrands, R. L. Stamps, and M. P. Kostylev, Realization of spin-wave logic gates, Appl. Phys. Lett. **92**, 022505 (2008).

[13] M. Jamali, J. H. Kwon, S.-M. Seo, K.-J. Lee, and H. Yang, Spin wave nonreciprocity for logic device applications, Sci. Rep. **3**, 3160 (2013).

[14] A. Mahmoud, F. Ciubotaru, F. Vanderveken, A. V. Chumak, S. Hamdioui, C. Adelmann, and S. Cotofana, Introduction to spin wave computing, J. Appl. Phys. **128**, 161101 (2020).

[15] R. E. Camley, Z. Celinski, T. Fal, A. V. Glushchenko, A. J. Hutchison, Y. Khivintsev, B. Kuanr, I. R. Harward, V. Veerakumar, and V. V. Zagorodnii, High-frequency signal processing using magnetic layered structures, J. Magn. Magn. Mater. **321**, 2048 (2009).

[16] S. A. Nikitov, D. V. Kalyabin, I. V. Lisenkov, A. N. Slavin, Y. N. Barabanenkov, S. A. Osokin, A. V. Sadovnikov, E. N. Beginin, M. A. Morozova, Y. P. Sharaevsky, Y. A. Filimonov, Y. V. Khivintsev, S. L. Vysotsky, V. K. Sakharov, and E. S. Pavlov, Magnonics: A new research area in spintronics and spin wave electronics, Phys.–Usp. **58**, 1002 (2015).

[17] J.-V. Kim, R. L. Stamps, and R. E. Camley, Spin wave power flow and caustics in ultrathin ferromagnets with the Dzyaloshinskii-Moriya interaction, Phys. Rev. Lett.

117, 197204 (2016).
[18] B. W. Zingsem, M. Farle, R. L. Stamps, and R. E. Camley, Unusual nature of confined modes in a chiral system: Directional transport in standing waves, Phys. Rev. B **99**, 214429 (2019).
[19] C. Quispe Flores, C. Chalifour, J. Davidson, K. L. Livesey, and K. S. Buchanan, Semianalytical approach to calculating the dynamic modes of magnetic vortices with Dzyaloshinskii-Moriya interactions, Phys. Rev. B **102**, 024439 (2020).
[20] A. A. Stashkevich, M. Belmeguenai, Y. Roussigné, S. M. Cherif, M. Kostylev, M. Gabor, D. Lacour, C. Tiusan, and M. Hehn, Experimental study of spin-wave dispersion in Py/Pt film structures in the presence of an interface Dzyaloshinskii-Moriya interaction, Phys. Rev. B **91**, 214409 (2015).
[21] H. T. Nembach, J. M. Shaw, M. Weiler, E. Jué, and T. J. Silva, Linear relation between Heisenberg exchange and interfacial Dzyaloshinskii-Moriya interaction in metal films, Nat. Phys. **11**, 825 (2015).
[22] J.-H. Moon, S.-M. Seo, K.-J. Lee, K.-W. Kim, J. Ryu, H.-W. Lee, R. D. McMichael, and M. D. Stiles, Spin-wave propagation in the presence of interfacial Dzyaloshinskii-Moriya interaction, Phys. Rev. B **88**, 184404 (2013).
[23] D. Cortés-Ortuño and P. Landeros, Influence of the Dzyaloshinskii–Moriya interaction on the spin-wave spectra of thin films, J. Phys.: Condens. Matt. **25**, 156001 (2013).
[24] X. Wang, A. R. Stuart, M. S. Swyt, C. M. Q. Flores, A. T. Clark, A. Fiagbenu, R. V. Chopdekar, P. N. Lapa, Z. Xiao, D. Keavney, R. Rosenberg, M. Vogel, J. E. Pearson, S. G. E. te Velthuis, A. Hoffmann, K. S. Buchanan, and X. M. Cheng, Topological spin memory of antiferromagnetically coupled skyrmion pairs in Co/Gd/Pt multilayers, Phys. Rev. Mater. **6**, 084412 (2022).
[25] B. J. Kirby, H. F. Belliveau, D. D. Belyea, P. A. Kienzle, A. J. Grutter, P. Riego, A. Berger, and C. W. Miller, Spatial evolution of the ferromagnetic phase transition in an exchange graded film, Phys. Rev. Lett. **116**, 047203 (2016).
[26] M. Kostylev, Interface boundary conditions for dynamic magnetization and spin wave dynamics in a ferromagnetic layer with the interface Dzyaloshinskii-Moriya interaction, J. Appl. Phys. **115**, 233902 (2014).
[27] G. T. Rado and J. R. Weertman, Spin-wave resonance in a ferromagnetic metal, J. Phys. Chem. Solids **11**, 315 (1959).
[28] H. Puszkarski, Theory of interface magnons in magnetic multilayer films, Surf. Sci. Rep. **20**, 45 (1994).
[29] M. Buchmeier, B. K. Kuanr, R. R. Gareev, D. E. Bürgler, and P. Grünberg, Spin waves in magnetic double layers with strong antiferromagnetic interlayer exchange coupling: Theory and experiment, Phys. Rev. B **67**, 184404 (2003).
[30] R. L. Stamps and R. E. Camley, Spin waves in antiferromagnetic thin films and multilayers: Surface and interface exchange and entire-cell effective-medium theory, Phys. Rev. B **54**, 15200 (1996).
[31] K. L. Livesey, D. C. Crew, and R. L. Stamps, Spin wave valve in an exchange spring bilayer, Phys. Rev. B **73**, 184432 (2006).
[32] T. Moore, R. E. Camley, and K. L. Livesey, Spin waves in a thin film with magnetoelectric coupling at the surfaces, J. Magn. Magn. Mater. **372**, 107 (2014).
[33] Z. Yang, C. Liu, X. Yang, and Y. Zhang, Influence of local Dzyaloshinskii-Moriya interaction on spin waves in symmetrical heavy metal/ferromagnet/heavy metal multilayer, J. Phys. D: Appl. Phys. **58**, 03LT03 (2024).
[34] O. Gladii, M. Haidar, Y. Henry, M. Kostylev, and M. Bailleul, Frequency nonreciprocity of surface spin wave in permalloy thin films, Phys. Rev. B **93**, 054430 (2016).
[35] K. Szulc, J. Kharlan, P. Bondarenko, E. V. Tartakovskaya, and M. Krawczyk, Impact of surface anisotropy on the spin-wave dynamics in a thin ferromagnetic film, Phys. Rev. B **109**, 054430 (2024).
[36] S. Blumenröder, E. Zirngiebl, P. Grünberg, and G. Güntherodt, Observation of standing spin waves in thin Fe films by means of Raman spectroscopy, J. Appl. Phys. **57**, 3684 (1985).
[37] P. M. Yarbrough, K. L. Livesey, R. E. Camley, and R. Macêdo, Far-infrared reflection from heterostructures made of ultrathin ferromagnetic layers, Phys. Rev. Appl. **12**, 024004 (2019).
[38] A. Soumyanarayanan, M. Raju, A. L. Gonzalez Oyarce, A. K. C. Tan, M.-Y. Im, A. P. Petrović, P. Ho, K. H. Khoo, M. Tran, C. K. Gan, F. Ernult, and C. Panagopoulos, Tunable room-temperature magnetic skyrmions in Ir/Fe/Co/Pt multilayers, Nat. Mater. **16**, 898 (2017).
[39] A. W. J. Wells, P. M. Shepley, C. H. Marrows, and T. A. Moore, Effect of interfacial intermixing on the Dzyaloshinskii-Moriya interaction in Pt/Co/Pt, Phys. Rev. B **95**, 054428 (2017).
[40] Y. Ishikuro, M. Kawaguchi, N. Kato, Y.-C. Lau, and M. Hayashi, Dzyaloshinskii-Moriya interaction and spin-orbit torque at the Ir/Co interface, Phys. Rev. B **99**, 134421 (2019).
[41] P. Jadaun, L. F. Register, and S. K. Banerjee, The microscopic origin of DMI in magnetic bilayers and prediction of giant DMI in new bilayers, Npj Comput. Mater. **6**, 88 (2020).
[42] M. Vaňatka, K. Szulc, O. Wojewoda, C. Dubs, A. V. Chumak, M. Krawczyk, O. V. Dobrovolskiy, J. W. Kłos, and M. Urbánek, Spin-wave dispersion measurement by variable-gap propagating spin-wave spectroscopy, Phys. Rev. Appl. **16**, 054033 (2021).
[43] J. Qi, Y. Zhao, H. Huang, Y. Zhang, H. Lyu, G. Yang, J. Zhang, B. Shao, K. Jin, Y. Zhang, H. Wei, B. Shen, and S. Wang, Tailoring of the interfacial Dzyaloshinskii–Moriya interaction in perpendicularly magnetized epitaxial multilayers by crystal engineering, J. Phys. Chem. Lett. **14**, 637 (2023).
[44] R. E. Hummel, *Electronic properties of materials* (Springer Science & Business Media, New York, 2011).
[45] C. A. F. Vaz, J. A. C. Bland, and G. Lauhoff, Magnetism in ultrathin film structures, Rep. Prog. Phys. **71**, 056501 (2008).
[46] O. Gladii, D. Halley, Y. Henry, and M. Bailleul, Spin-wave propagation and spin-polarized electron transport in single-crystal iron films, Phys. Rev. B **96**, 174420 (2017).
[47] I. Benguettat-El Mokhtari, D. Ourdani, Y. Roussigne, R. B. Mos, M. Nasui, F. Kail, L. Chahed, S. M. Chérif, A. Stashkevich, M. Gabor, and M. Belmeguenai, Perpendicular magnetic anisotropy and interfacial Dzyaloshinskii–Moriya interaction in as grown and annealed X/Co/Y ultrathin systems, J. Phys.: Condens. Matter **32**, 495802 (2020).

[48] F. Schreiber and Z. Frait, Spin-wave resonance in high-conductivity films: The Fe-Co alloy system, Phys. Rev. B **54**, 6473 (1996).

[49] S. Heinze, K. Von Bergmann, M. Menzel, J. Brede, A. Kubetzka, R. Wiesendanger, G. Bihlmayer, and S. Blügel, Spontaneous atomic-scale magnetic skyrmion lattice in two dimensions, Nat. Phys. **7**, 713 (2011).

[50] I. A. Golovchanskiy, I. V. Yanilkin, A. I. Gumarov, B. F. Gabbasov, N. N. Abramov, R. V. Yusupov, R. I. Khaibullin, and L. R. Tagirov, Exchange spin waves in thin films with gradient composition, Phys. Rev. Mater. **6**, 064406 (2022).

[51] B. Assouline, M. Brik, N. Bernstein, and A. Capua, Amplification of electron-mediated spin currents by stimulated spin pumping, Phys. Rev. Res. **4**, L042014 (2022).